OPEN ACCESS
CellPress

Cell Reports
Article

ATP-Dependent Lon Protease Controls Tumor Bioenergetics by Reprogramming Mitochondrial Activity

Pedro M. Quirós,[1] Yaiza Español,[1] Rebeca Acín-Pérez,[2] Francisco Rodríguez,[1] Clea Bárcena,[1] Kenta Watanabe,[1] Enrique Calvo,[3] Marta Loureiro,[3] M. Soledad Fernández-García,[4] Antonio Fueyo,[5] Jesús Vázquez,[3] José Antonio Enríquez,[2] and Carlos López-Otín[1,*]

[1]Departamento de Bioquímica y Biología Molecular, Facultad de Medicina, Instituto Universitario de Oncología, Universidad de Oviedo, 33006 Oviedo, Spain
[2]Department of Cardiovascular Development and Repair, Centro Nacional de Investigaciones Cardiovasculares, 28029 Madrid, Spain
[3]Cardiovascular Proteomics Laboratory, Department of Vascular Biology, Centro Nacional de Investigaciones Cardiovasculares, 28029 Madrid, Spain
[4]Servicio de Anatomía Patológica, Hospital Universitario Central de Asturias, 33006 Oviedo, Spain
[5]Area de Fisiología, Departamento de Biología Funcional, Facultad de Medicina, Instituto Universitario de Oncología, Universidad de Oviedo, 33006 Oviedo, Spain
*Correspondence: clo@uniovi.es
http://dx.doi.org/10.1016/j.celrep.2014.06.018

SUMMARY

We generated mice deficient in Lon protease (LONP1), a major enzyme of the mitochondrial quality control machinery. Homozygous deletion of *Lonp1* causes early embryonic lethality, whereas its haploinsufficiency protects against colorectal and skin tumors. Furthermore, LONP1 knockdown inhibits cellular proliferation and tumor and metastasis formation, whereas its overexpression increases tumorigenesis. Clinical studies indicate that high levels of *LONP1* are a poor prognosis marker in human colorectal cancer and melanoma. Additionally, functional analyses show that LONP1 plays a key role in metabolic reprogramming by remodeling OXPHOS complexes and protecting against senescence. Our findings demonstrate the relevance of LONP1 for cellular and organismal viability and identify this protease as a central regulator of mitochondrial activity in oncogenesis.

INTRODUCTION

Mitochondria are subcellular organelles of eukaryotic cells responsible for generating the bulk of cellular energy in the form of ATP through oxidative phosphorylation (OXPHOS; Friedman and Nunnari, 2014). Mitochondria are also involved in other pathways of intermediate metabolism, generate and regulate reactive oxygen species (ROS), maintain homeostasis and calcium buffering, and participate in essential cellular processes such as apoptosis (Wallace et al., 2010). Consistent with the wide diversity of functional roles played by these organelles, mitochondrial dysfunctions are associated with aging and pathological processes such as cancer and neurological diseases (López-Otín et al., 2013; Wallace, 2005). To exert their functions properly, mitochondria have developed a quality control system composed of proteases and chaperones that regulate the assembly, folding, and turnover of proteins, as well as the removal of damaged proteins (Tatsuta, 2009). In mammals, there are four major ATP-dependent proteases that participate in mitochondrial quality control: Yme1 and m-AAA proteases localized in the inner membrane, and ClpP and Lon located in the matrix (Rugarli and Langer, 2012). Additionally, there are several ATP-independent proteases that collaborate in mitochondrial homeostasis (Cipolat et al., 2006; Quirós et al., 2012).

Lon protease (LONP1) is a conserved serine peptidase that contributes to protein quality control processes from bacteria to eukaryotic cells (Lu et al., 2003). LONP1 plays an important role in the degradation of misfolded and damaged proteins, and supports cell viability under oxidative, hypoxic, and endoplasmic reticulum-stress conditions (Venkatesh et al., 2012). There are several proposed substrates for this enzyme in mammals, such as aconitase, cytochrome c oxidase isoform COX4-1, steroidogenic acute regulatory protein, and 5-aminolevulinic acid synthase (Bota and Davies, 2002; Fukuda et al., 2007; Granot et al., 2007; Tian et al., 2011). LONP1 is also a DNA-binding protein that participates in mtDNA maintenance and gene expression regulation (Liu et al., 2004). Moreover, LONP1 degrades mitochondrial transcription factor A (TFAM), regulating mtDNA copy number and metabolism to maintain the TFAM/mtDNA ratio necessary to control replication and transcription (Lu et al., 2013; Matsushima et al., 2010).

Consistent with the crucial role of LONP1 in the control of mitochondrial function under stress conditions, changes in the expression levels of this protease gene are associated with several human diseases (Venkatesh et al., 2012). Moreover, LONP1 levels are increased in different tumors and tumor cell lines (Bernstein et al., 2012; Hu et al., 2005; Kita et al., 2012). Interestingly, downregulation of *LONP1* in some tumor cells causes apoptosis and cell death (Bota et al., 2005), indicating

a possible addiction of tumor cells to LONP1 function, as occurs with other intracellular proteases associated with cancer (Fraile et al., 2012; Freije et al., 2011).

To further analyze the in vivo roles of this mitochondrial protease in both normal and pathological conditions, including cancer, we have generated mutant mice deficient in Lonp1. Homozygous deletion of *Lonp1* causes early embryonic lethality but *Lonp1*$^{+/-}$ heterozygous mice are fertile and viable, thereby facilitating cancer susceptibility studies that have shown that these haploinsufficient animals are protected against colon and skin carcinomas induced by chemical carcinogens. Moreover, knockdown of Lon protease in colorectal and melanoma cells inhibits in vivo tumor growth and metastasis, respectively, whereas *LONP1* overexpression promotes tumorigenesis. Finally, we provide evidence that LONP1 regulates metabolic reprogramming and controls tumor bioenergetics by remodeling OXPHOS complexes.

RESULTS

Lonp1 Deletion Causes Embryonic Lethality in Mice

Mice heterozygous for the targeted allele of the mitochondrial Lon protease (*Lonp1*$^{+/-}$) were viable and fertile with no obvious abnormalities. These mice were intercrossed to generate homozygous mice deficient in *Lonp1* (Figure S1A). However, we did not detect homozygous pups at weaning (Figure S1B), suggesting that *Lonp1* homozygous deletion causes embryonic lethality. To further assess this hypothesis, we analyzed and genotyped embryos at different stages of development, from 3.5 to 9.5 days postcoitum (dpc). We found that at blastocyst stage (3.5 dpc), the number of embryos of the different genotypes followed the expected Mendelian ratios. However, at 8.5 dpc, only one of the analyzed viable embryos carried the homozygous mutation, whereas at 9.5 dpc none of them carried the mutation in homozygosis (Figures 1A and S1B). Moreover, analysis of nonviable mutant embryos at 8.5 dpc showed a clear reduction in size when compared with their littermate controls, looking like 7.5 dpc embryos and suggesting that their development was arrested. These differences were maintained at 9.5 dpc (Figure 1A). To clarify the embryonic lethality of *Lonp1*$^{-/-}$, we performed comparative histological analysis of embryos from both genotypes. *Lonp1*$^{-/-}$ embryos from 5.5 and 6.5 dpc showed normal size and development (Figure 1B). However, at 7.5 dpc, *Lonp1* null embryos showed a marked growth decrease, being much smaller than their littermate controls and exhibiting incomplete formation of embryo cavities, thereby pointing to a developmental arrest at the egg-cylinder early gastrulation stage (Figure 1B).

To further characterize the cause of lethality observed in *Lonp1* null embryos, we first tried to generate ES cells or murine embryonic fibroblasts with homozygous deletion of *Lonp1*. However, after repeated experiments, we were unable to obtain any *Lonp1*-deficient cell line. To evaluate the putative relationship between mtDNA deficiencies and embryonic lethality in *Lonp1* null mice, we analyzed mtDNA copy number in *Lonp1*-null embryos during development. We observed that at 3.5 dpc, there were no differences between control, heterozygous, and *Lonp1* null embryos (Figure 1C). However, analysis at 7.5 dpc showed a decrease in mtDNA copy number in *Lonp1*-deficient embryos compared with control and heterozygous embryos (Figure 1C). To further evaluate the influence of LONP1 deficiency in embryo development, we analyzed the in vitro growth of embryos. We isolated preimplantation embryos by uterine flushing at the blastocyst stage (3.5 dpc). As shown in Figures 1D and S1B, almost all blastocysts obtained from intercrossed heterozygous mice were normal and viable, and *Lonp1*-null blastocysts were indistinguishable from the corresponding controls. We then cultured blastocysts for 5 days in embryonic stem cell media, finding that virtually all analyzed embryos developed normally. However, *Lonp1*-deficient embryos showed a smaller size in the inner cell mass and trophoblast cells compared with littermates (Figure 1E). Taken together, these results indicate that LONP1 is essential for in vivo and in vitro embryo development. Embryonic absence of this protease leads to marked growth retardation and arrest likely due to mitochondrial dysfunction and loss of mtDNA, with subsequent failure to accomplish the energy requirements necessary for embryonic development.

In marked contrast to embryonic lethality of *Lonp1*$^{-/-}$ mice, *Lonp1*$^{+/-}$ animals developed normally and did not display any obvious pathological alterations. Analysis of *Lonp1* expression in heterozygous mice indicated a 50% reduction at both RNA and protein levels in these animals (Figures 1F and 1G). These findings demonstrate that LONP1 haploinsufficiency is compatible with embryonic and adult mouse development, as well as with normal growth and fertility, thus opening the possibility to perform long-term studies of cancer susceptibility in *Lonp1*$^{+/-}$ mice.

Lonp1-Haploinsufficient Mice Are Protected against Colorectal Cancer and Chemically Induced Skin Tumors

To analyze the role of LONP1 in tumor development, we induced colon carcinoma in *Lonp1*$^{+/-}$ and *Lonp1*$^{+/+}$ mice, using azoxymethane (AOM) and dextrane sulfate (Figure 2A). All *Lonp1* wild-type mice, but only 72% *Lonp1* heterozygous mice, developed colorectal tumors (Figure 2B). Moreover, *Lonp1*$^{+/-}$ mice had significantly fewer tumors than control animals (Figures 2C and 2D). There was also a decrease in the colon length in *Lonp1* control mice compared with heterozygous mice (Figure 2E). Quantitative analysis of the clinical score during the carcinogenesis protocol revealed that *Lonp1*$^{+/-}$ mice exhibited milder clinical features than wild-type animals (Figure 2F).

To characterize the putative role of LONP1 in tumor development, we used an additional carcinogenesis protocol to induce skin tumors. We subjected *Lonp1*-heterozygous mice and their wild-type littermate controls to a 7,12-dimethylbenzanthracene and tetradecanoylphorbol acetate (DMBA/TPA) protocol that induces skin papillomas. *Lonp1* heterozygous mice developed significantly fewer and smaller papillomas during the treatment and displayed a significantly lower incidence of the appearance of papillomas (Figures 2G–2I). These results indicate that LONP1 has a key role in the development of colon and skin tumors, and a decrease in Lonp1 levels protects against colorectal carcinoma and papilloma formation in mice.

LONP1 Is Upregulated in Colon Cancer and Promotes Tumor Growth

To clarify the role of this mitochondrial protease in colorectal cancer, we studied *LONP1* expression in different human

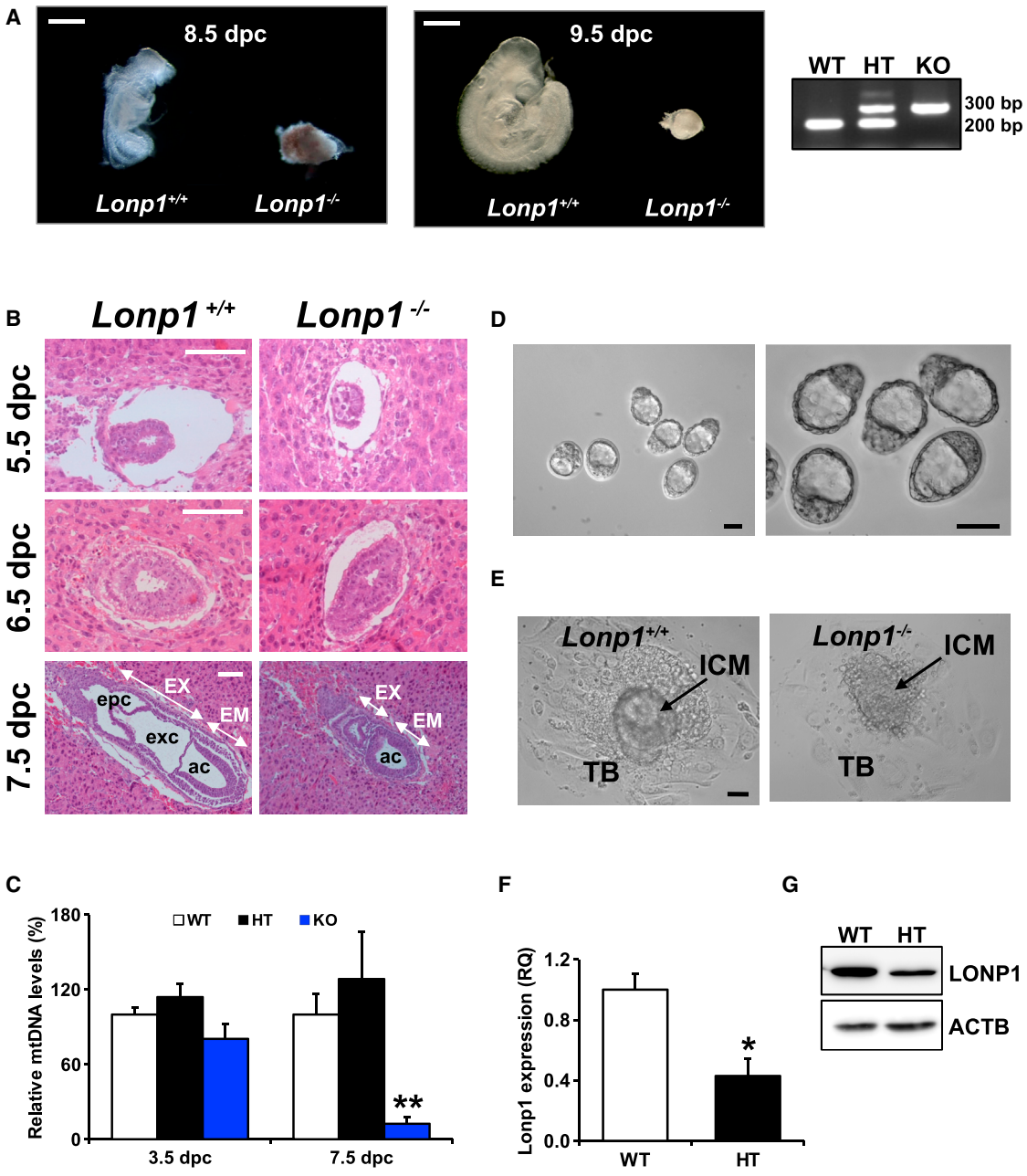

Figure 1. *Lonp1* Deletion Causes Embryonic Lethality

(A) Representative images of *Lonp1*$^{+/+}$ and *Lonp1*$^{-/-}$ embryos at 8.5 and 9.5 dpc. Scale bar represents 1 mm. Right: PCR analysis of Lonp1 embryos' genotypes.

(B) Histological analysis of embryos from 5.5 to 7.5 dpc of control and *Lonp1*-deficient embryos. EX, extraembryonic part; EM, embryonic part; epc, ectoplacental cavity; exc, exocoelomic cavity; ac, amniotic cavity. Scale bar represents 100 μm.

(C) Analysis of mtDNA quantity expressed as a percentage of levels in control embryos at 3.5 dpc and 7.5 dpc embryos. Data are presented as mean ± SEM (n = 10–20), **p < 0.01.

(D) Representative images of blastocysts (3.5 dpc embryos) obtained after heterozygous intercrosses of *Lonp1* mice.

(E) *Lonp1*-null embryos showed reduced size and delayed development in vitro compared with control blastocysts. ICM, inner cell mass; TB, trophoblastic cells. Scale bar represents 50 μm.

(F) qPCR and (G) western blot analysis of *LONP1* expression in murine embryonic fibroblasts derived from *Lonp1*$^{+/+}$ and *Lonp1*$^{+/-}$ mice. qPCR data are presented as RQ value ± SD, **p < 0.01.

colorectal cancer cell lines (HCT116, HCT15, HT29, SW480, SW620, DLD-1, and RKO), and in a colon epithelial cell line (FHC). Quantitative PCR and western blot analysis showed a high expression of *LONP1* in all colon cancer cell lines compared to the control epithelial colon cells (Figures 3A and 3B). To analyze the relevance of Lon protease in these colon carcinoma cells, we used HCT116 cells to perform in vitro and in vivo studies of loss- and gain-of-function. We reduced Lon protease levels using lentiviral-based shRNAs against LONP1, and ectopically induced LONP1 using a retroviral system that expresses a Flag-tagged LONP1 cDNA construct. The expression of LONP1 was confirmed with qPCR and western blot analysis (Figures 3C and S2A). Knockdown of LONP1 (shLon) significantly reduced cell proliferation in vitro compared to control cells (pLKO1; Figures 3D and S2B). However, ectopic expression of LONP1 (LON) did not increase proliferation when compared to control cells (pMX; Figure 3D). Likewise, overexpression of LONP1 in DLD-1, a colon cancer cell line with low levels of LONP1 expression, did not increase the proliferation rates (Figure S2C). We then examined the in vivo relevance of LONP1 expression on tumor growth, using a xenograft model. As shown in Figure 3E, tumor growth of shLon cells was significantly reduced when compared to pLKO1 control cells. On the other hand, ectopic expression of LONP1 increased growth of tumors in nude mice compared to those generated by pMX control cells (Figure 3F). These results indicate that LONP1 is necessary to maintain the proliferative rates and tumor growth of this colorectal cancer cell line.

To further evaluate the relevance of *LONP1* expression in colon carcinoma, we performed an immunohistochemical analysis of human samples from normal and tumor colorectal sections. In agreement with previous data, *LONP1* is expressed in normal colon samples and highly upregulated in colon cancer mucosa (Figure 3G). Moreover, analysis of transcriptional data from colorectal adenomas and normal mucosa showed a significant increase in *LONP1* expression in adenomas compared to their matched normal mucosa (Figure 3H). Detailed analysis of reported data on survival of patients with Duke's stages A–C colorectal carcinoma showed a positive correlation between high *LONP1* expression and lower survival (Figure 3I). Collectively, these results suggest that Lonp1 upregulation is common in colorectal cancer and may provide some advantage to tumor cells, thereby facilitating cancer development.

LONP1 Is Necessary for Proliferation and Metastasis of Melanoma Cells

As described above, *Lonp1*-heterozygous mice displayed less susceptibility to develop tumors than control mice. Analysis of human cutaneous melanoma, showed a significant increase in *LONP1* levels in melanoma compared to normal skin or benign nevi samples (Figure 4A). Moreover, analysis of clinical outcome of patients with metastatic melanoma showed a positive correlation between *LONP1* expression and short survival (Figure 4B). To further evaluate the functional relevance of Lon protease in tumor and metastasis formation in vivo, we used the murine B16F10 melanoma cells in which we reduced LONP1 levels using lentiviral-based shRNA and induced ectopic expression of LONP1 using a retroviral system. A complete set of shRNA (shLon) reduced both LONP1 mRNA and protein levels approximately 90% compared with control pLKO1 shRNA, whereas ectopic expression of Lon increased the levels of protein and mRNA 10-fold (Figures 4C, 4D, and S3A). Knockdown of LONP1 diminished in vitro proliferation of B16F10 cells, whereas ectopic expression of LONP1 did not increase proliferation rates (Figures 4E and S3A). We then analyzed the in vivo formation of experimental lung metastasis using this highly metastatic melanoma cell line. As shown in Figure 4F, knockdown of LONP1 reduced 10-fold the number of metastasis compared to pLKO1 control cells. Conversely, overexpression of Lon protease increased significantly the number of metastasis (Figure 4G). These results indicate that LONP1 is essential for cell proliferation as well as for metastasis formation in vivo, and high levels of *LONP1* are a marker of poor prognosis in human melanoma.

LONP1 Induces a Metabolic Switch and Regulates Tumor Bioenergetics by Remodeling OXPHOS Complexes

To study the role of LONP1 in the regulation of mitochondrial function in cancer, we used the above described B16F10 melanoma cells with knockdown or overexpression of Lon protease. These melanoma cells are wild-type for BRAF, indicating that the mitochondrial activity and respiration are important and the energy production is not shifted to glycolysis (Castle et al., 2012; Haq et al., 2013). Knockdown of LONP1 decreased cellular ATP content, whereas ectopic expression of LONP1 increased ATP content (Figures 5A and S4A). Furthermore, analysis of mitochondrial respiration showed a decrease in basal oxygen consumption in LONP1 ablated cells when compared to controls (Figures 5B and S4B). Interestingly, overexpression of Lon protease also showed a decrease in mitochondrial respiration compared to control cells (Figure 5B). Stimulation with the chemical uncoupler trifluorocarbonylcyanide phenylhydrazone increased oxygen consumption to maximal respiration rate in both pLKO1 and pMX control cells. Nevertheless, neither knockdown nor overexpression of Lon protease reached similar oxygen consumptions than control cells (Figures 5B and S4B). In addition, both knockdown and ectopic expression of LONP1 increased the glucose consumption and lactate production compared to controls (Figures 5C, 5D, S4C, and S4D). These results were puzzling because both conditions, i.e., ablation and overexpression of LONP1, induce the downregulation of respiration and the upregulation of the glycolytic pathway. To try to understand this phenomenon, we examined mitochondrial respiratory complexes and detected a significant decrease in complex I (Figures 5E and S4E) and a concomitant decrease in complex III-containing supercomplexes (Figures 5F and S4E) in shLon cells. Similarly, we observed a significant decrease in complex I, II, and IV in cells overexpressing LONP1 (Figures 5G and S4F), as well as a reduction in complex III-containing supercomplexes (Figures 5H and S4F). We also noticed that the relative amount of complex V in dimers was reduced in both models (Figures 5F and 5H). The observed decrease in mitochondrial complexes in both models likely derives from enhanced degradation or from a reduction in their assembly and could underlie the decrease in mitochondrial respiration in both *LONP1*-overexpressing and *LONP1*-deficient cells.

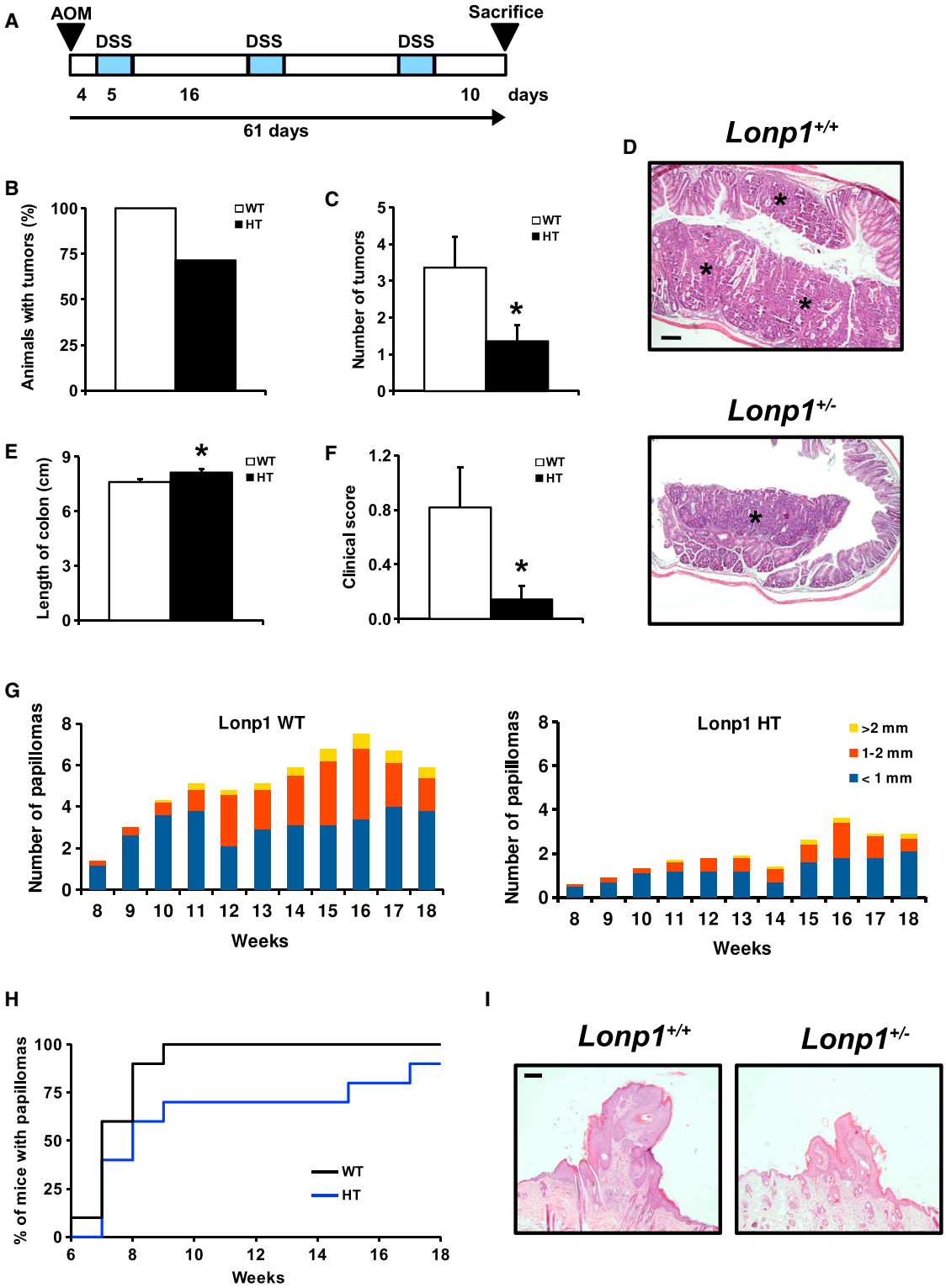

Figure 2. *Lonp1*$^{+/-}$ Mice Display Less Susceptibility to Azoxymethane-Induced Colon Tumors and Skin Chemical Carcinogenesis Induced by DMBA/TPA

(A) Scheme of azoxymethane-induced colon tumor protocol.

(B) Percentage of animals with tumors ($p < 0.05$).

(C) Average of tumors observed in *Lonp1*$^{+/+}$ and *Lonp1*$^{+/-}$ mice.

(legend continued on next page)

We next evaluated the individual activities of mitochondrial complexes by spectrophotometric analysis of mitochondria isolated from both cells. We observed that shLon cells showed significantly lower activities of complex I (CI) and combined complex II+complex III (CII+III) activity (Table S1), consistent with the low levels of CI and assembled CIII measured by BNGE (Figures 5E and 5F). In contrast, overexpression of LONP1 decreased almost all individual complex activities. Thus, we observed a reduction in CII and complex IV (CIV), as well as combined CI+III and CII+III activities (Table S1), consistent with the general decrease in almost all complexes observed by BNGE (Figures 5G and 5H). Moreover, knockdown of Lon protease specifically induced an increased activity of CI+III relative to CI (CI+III/CI) and decreased activity of CII+III relative to CII (CII+III/CII) (Figure 5I), suggesting that complex III is more dedicated to complex I than to complex II, favoring the use NADH equivalents and the respiration through complex I. However, overexpression of Lon protease showed a decrease in the activity of CI+III relative to CI (CI+III/CI), which indicated a reduction in the respiration through complex I, while respiration efficiency through complex II (CII+III/CII) remained unaltered (Figure 5J). Collectively, the changes observed in the *LONP1*-overexpressing cells are consistent with a metabolic reprogramming of the OXPHOS system by primarily reducing the flux from NADH electrons (more catabolic), but maintaining the flux through the FAD-dependent enzymes, that are also involved in anabolic (nucleotide and amino acid metabolism) and detoxifying metabolic pathways. Nevertheless, the changes in respiration flux observed in shLon cells are more closely related to a catabolic metabolism.

To further clarify the differences observed in the regulation of OXPHOS complexes in *LONP1*-overexpressing and *LONP1*-knockdown cells, we performed a quantitative proteomic analysis, using iTRAQ labeling and subsequent LC-MS/MS analysis. As an internal control of our analysis, we found a significant increase in LONP1 protein levels in the overexpression model, whereas this protease was undetectable in the downregulation model (Figure 5K). Consistent with the above findings in OXPHOS complex levels, we detected a significant alteration in the amount of complex I proteins in both *LONP1*-overexpressing and *LONP1*-knockdown cells (Figure 5K). However, the affected complex I protein components differed between both cells, suggesting a distinct mechanism of regulation in each condition. Thus, all CI proteins were downregulated in *LONP1*-knockdown cells, while they presented variability in *LONP1*-overexpressing cells, some of them being upregulated and other downregulated. Furthermore, CI structural proteins, such as NDUFB6, 8, 10 and 11, were the more downregulated proteins in *LONP1*-knockdown cells, while they were upregulated in *LONP1*-overexpressing cells. Importantly, these proteins are associated with the assembly and stability of the CI membrane domains and are required for their activity (Andrews et al., 2013; Perales-Clemente et al., 2010). Conversely, among the most decreased proteins in the *LONP1*-overexpressing cells, there were four subunits of the NADH dehydrogenase and hydrogenase catalytic modules of CI, such as NDUFV1, NDUFV2, NDUFS3, and NDUFS7. Interestingly, it has been described that these proteins can be removed and replaced in the complex I without degrading the whole complex (Dieteren et al., 2012; Lazarou et al., 2007). These results indicate that the observed complex I decrease in shLon cells was a consequence of loss of stability of this complex, whereas in *LONP1*-overexpressing cells the decrease was functional, maintaining the structural domains. Moreover, complex V subunits were clearly downregulated in shLon cells (Figure 5K), which is in line with the observed decrease in complex V dimers (Figure 5F). Interestingly, *LONP1*-overexpressing cells showed an increase in complex V subunits (Figure 5K), despite the observed decrease in dimers (Figure 5H), which indicates that these cells have a different complex V regulation.

Overall, these data strongly suggest that the apparent convergence in the decrease in aerobic respiration and the subsequent glycolysis activation, by either knockdown or overexpression of LONP1, takes place through different mechanisms. The loss of mitochondrial complexes would operate in shLon cells, whereas OXPHOS complexes remodeling would underlie the alterations found in *LONP1*-overexpressing cells.

LONP1 Keeps Mitochondrial Function and Induces a Global Metabolic Reprogramming

To further clarify the observed alterations in *LONP1*-overexpressing and *LONP1*-knockdown cells, we analyzed other parameters related to mitochondrial function in these cells. We first found that *LONP1*-knockdown, but not its overexpression, induced a decrease in both mitochondrial membrane potential (Figure 6A) and mtDNA content (Figure 6B). shLon cells also displayed an increase in mitochondrial fragmentation (Figures 6C and S5A) and ROS production (Figure 6D), which caused the proteolytic processing of OPA1 (Figures 6E and S5B). These findings are indicative of a clear mitochondrial dysfunction, which is not observed in *LONP1*-overexpressing cells. Moreover, knockdown of Lon protease activated the AMPK pathway (Figure 6E), which is in line with the low ATP levels and the mitochondrial stress scenario observed in these cells. In contrast, overexpression of *LONP1* decreased AMPK activation (Figure 6E). In addition, and consistent with the enhancement of the glycolytic pathway detected in both *LONP1*-overexpressing and *LONP1*-knockdown cells, there was an increase in the expression of glycolytic genes in both cases (Figure S5C).

(D) Representative images of hematoxylin and eosin staining of colon sections from $Lonp1^{+/+}$ and $Lonp1^{+/-}$ mice at the end of the experiment. Scale bar represents 200 μm.
(E) Measurement of the length of the colon at the end of the experiment.
(F) Clinical score throughout the experiment based on stool consistency and rectal bleeding. Data are presented as mean ± SEM (n = 11–14), *p < 0.05.
(G) Average number of papillomas per mouse grouped by size (diameter of the lesion in millimeters), and represented for each genotype (n = 10).
(H) Inverse Kaplan-Meier analysis of the percentage of mice with papillomas. Log-rank test p = 0.0439.
(I) Representative pictures of papilloma lesions of $Lonp1^{+/+}$ and $Lonp1^{+/-}$ at week 18. Scale bar represents 200 μm.

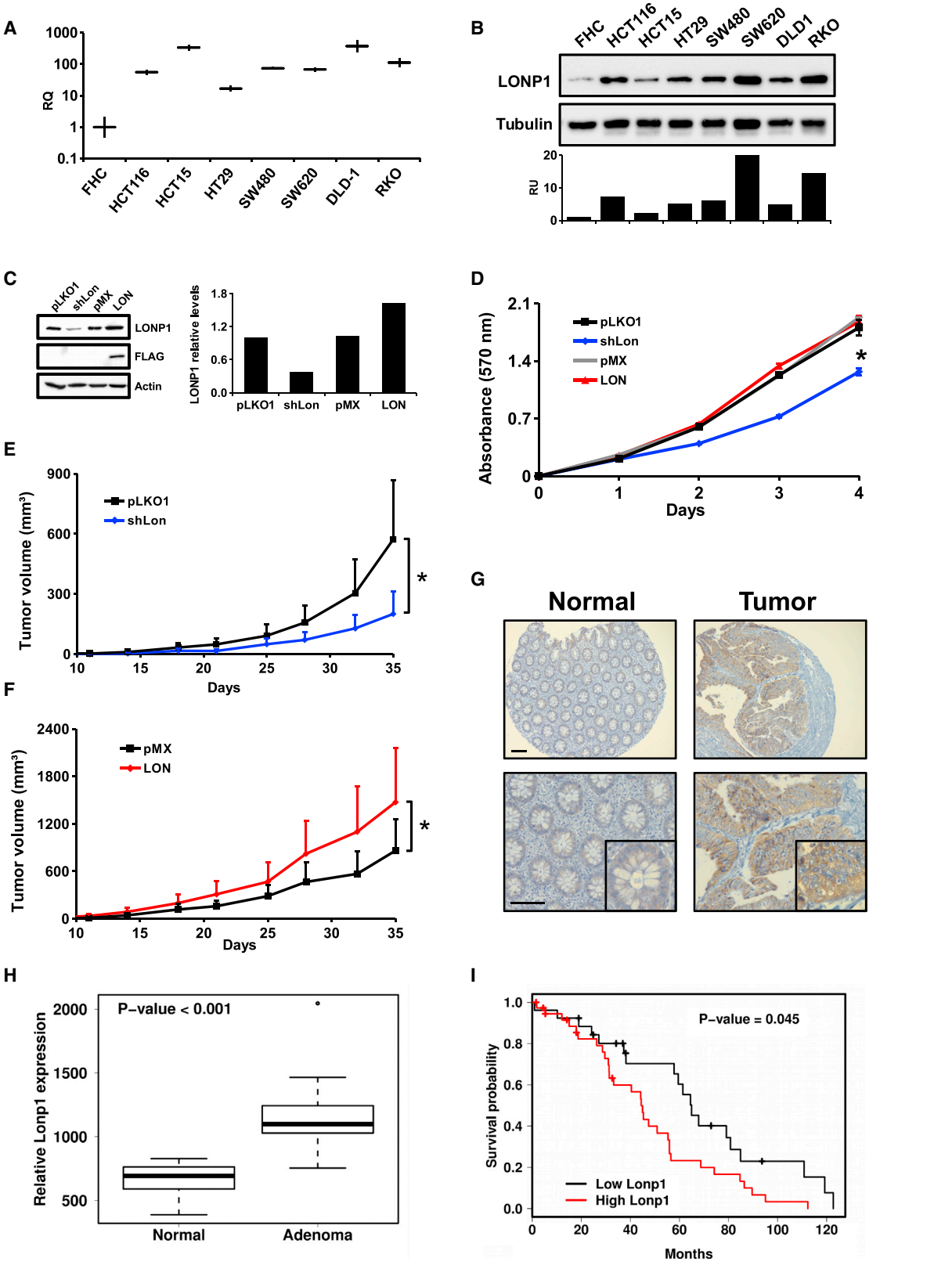

(legend on next page)

However, analysis of lipid synthesis showed a significant decrease in shLon cells, which agrees with the AMPK activation in these cells, whereas *LONP1*-overexpressing cells displayed similar rates than control cells (Figures 6F and S5D). Interestingly, and despite that we did not detect differences in apoptosis (data not shown), we found increased levels of the antiapoptotic protein Bcl-2 in *LONP1*-overexpressing cells and decreased levels in shLon cells (Figure 6E), which suggests a possible increase in apoptosis sensitivity in *LONP1*-deficient cells. We next examined in both *LONP1*-overexpressing and *LONP1*-knockdown cells the levels and activity of aconitase (ACO2), a well-established substrate for Lon protease. We found a decrease in ACO2 activity in *LONP1*-overexpressing cells and an increased activity of this enzyme in shLon cells (Figure S5E). The low expression levels of ACO2 in these cells precluded the detection of clear differences in enzyme levels. However, after transfection of a cDNA encoding ACO2, we detected increased levels and activity of this enzyme in control cells, but not in *LONP1*-overexpressing cells (Figures S5F and S5G), indicating that LONP1 processes ACO2 under conditions where this substrate is highly expressed.

Taken together, these results indicate that the absence of LONP1 induces a generalized mitochondrial dysfunction, whereas its overexpression does not alter the mitochondrial homeostasis. To further characterize the cellular alterations induced by the depletion and overexpression of LONP1, we performed quantitative proteomic analysis of the corresponding cells and found that *LONP1* overexpression increased the levels of proteins related with protein synthesis, such as eukaryotic translation initiation factor complex 3 and ribosomal proteins (Figure 6G). We also found increased levels of proteins related to the spliceosome, proteasome, and chaperone-containing T complex (Figure 6H), which is consistent with the increased tumorigenesis observed in *LONP1*-overexpressing cells. Conversely, *LONP1*-deficient cells showed reduced levels of all of these proteins (Figures 6G and 6H), which agrees well with the low proliferation rate and tumorigenic potential of these cells. These data illustrate the occurrence of marked differences in the process of metabolic adaptation after modulation of LONP1 levels, which leads to a profound mitochondrial dysfunction when cells are depleted of Lon protease and to a global metabolic remodeling when this mitochondrial enzyme is overexpressed.

LONP1 Contributes to Bypass Oncogene-Induced Senescence

LONP1 knockdown induces growth arrest and mitochondrial dysfunction in melanoma cells, impairing mitochondrial respiration and causing loss of mitochondrial integrity. Interestingly, we also observed that shLon cells displayed an increase in size compared with control pLKO1 or LONP1-overexpressing cells, suggesting the occurrence of a cellular senescence phenotype (Figure 7A). Moreover, β-galactosidase staining (a marker of senescent cells) showed an increased positivity in cells lacking Lonp1, whereas overexpression of LONP1 decreased the number of β-galactosidase positive cells (Figure 7B). The induction of cellular senescence is mainly mediated by signals derived from a permanent DNA damage response. Accordingly, we found that the loss of mitochondrial integrity caused by LONP1 deficiency induced a DNA damage response likely mediated by p53, as assessed by the increased levels of direct transcriptional targets of this tumor suppressor (Figure 7C). Interestingly, knockdown of LONP1 in *p53*-deficient cells resulted in lower proliferation defects when compared to wild-type cells, indicating that p53 contributes to the observed alterations (Figure 7D). Overexpression of LONP1 in B16F10 cells reduced the levels of these markers and β-galactosidase activity (Figures 7B and 7D), indicating a protection against senescence by Lon protease, which was consistent with the tumorigenic increase of these melanoma cells.

On the other hand, it is well established that mutations in *HRAS* or *BRAF* also induce a senescence phenotype, known as oncogene-induced senescence (OIS), as part of a cell response against tumor transformation (Michaloglou et al., 2005; Serrano et al., 1997). Based on this information, we explored available cancer transcriptome databases looking for putative differences in *LONP1* expression levels during OIS processes. Thus, by analyzing data from previous studies involving transformation of fibroblasts with mutant MEK, we found that induced OIS did not promote changes in *LONP1* expression. However, bypassing senescence in these fibroblasts using viral oncoproteins significantly increased *LONP1* expression (Figure 7E), further supporting the idea that upregulation of Lon protease may favor oncogenic transformation. These results demonstrate that LONP1 is essential to protect against senescence, and reinforce the proposal that levels of this serine protease contribute to modulate the tumorigenic properties of cancer cells.

Figure 3. LONP1 Is Upregulated in Colon Cancer Cell Lines and Colorectal Tumors and Promotes Tumorigenesis In Vivo

(A) qPCR analysis of *LONP1* expression in colon cancer cell lines, normalized to colon epithelial cells and represented with a RQ value ± SD.

(B) Western blot analysis and densitometry quantification of LONP1 expression in the same colon cancer cell lines.

(C) Western blot and densitometry quantification of HCT116 colon cancer cells transduced with *LONP1* shRNA vectors (shLon) or with the empty vector as a control (pLKO1), as well as with pMX expressing murine *LONP1* (LON) and the empty vector (pMX). LONP1 values correspond to the concomitant expression of endogenous and flagged transgene.

(D–F) MTT analysis showed decreased proliferation in shLon HCT116 cell lines when compared to control cells; data are presented as mean ± SEM, $^*p < 0.05$. Tumor xenograft experiments were carried out using HCT116 cells and comparing (E) shLon transduced cells versus pLKO1 control cells and (F) *LONP1*-overexpressing cells versus pMX control cells. Tumor volume was calculated for each group at the indicated times after cancer cell injection, and significant differences were assessed with a linear mixed-effects model; data are presented as mean ± SEM ($n = 7$), $^*p < 0.05$.

(G) Immunohistochemical analysis of LONP1 expression in normal and tumor colon human samples.

(H) Relative expression of *LONP1* extracted from a previously reported comparative data set of transcriptomes of 32 adenomas and those of normal mucosa from the same individuals (GEO accession number GDS2947) (Sabates-Bellver et al., 2007). Data are presented in box-and-whisker plot format.

(I) Kaplan-Meier survival curves for 64 patients with colorectal cancer expressing high (top 25% of patients) and low (bottom 25% of patients) *LONP1* levels. GSE14333 (Jorissen et al., 2009).

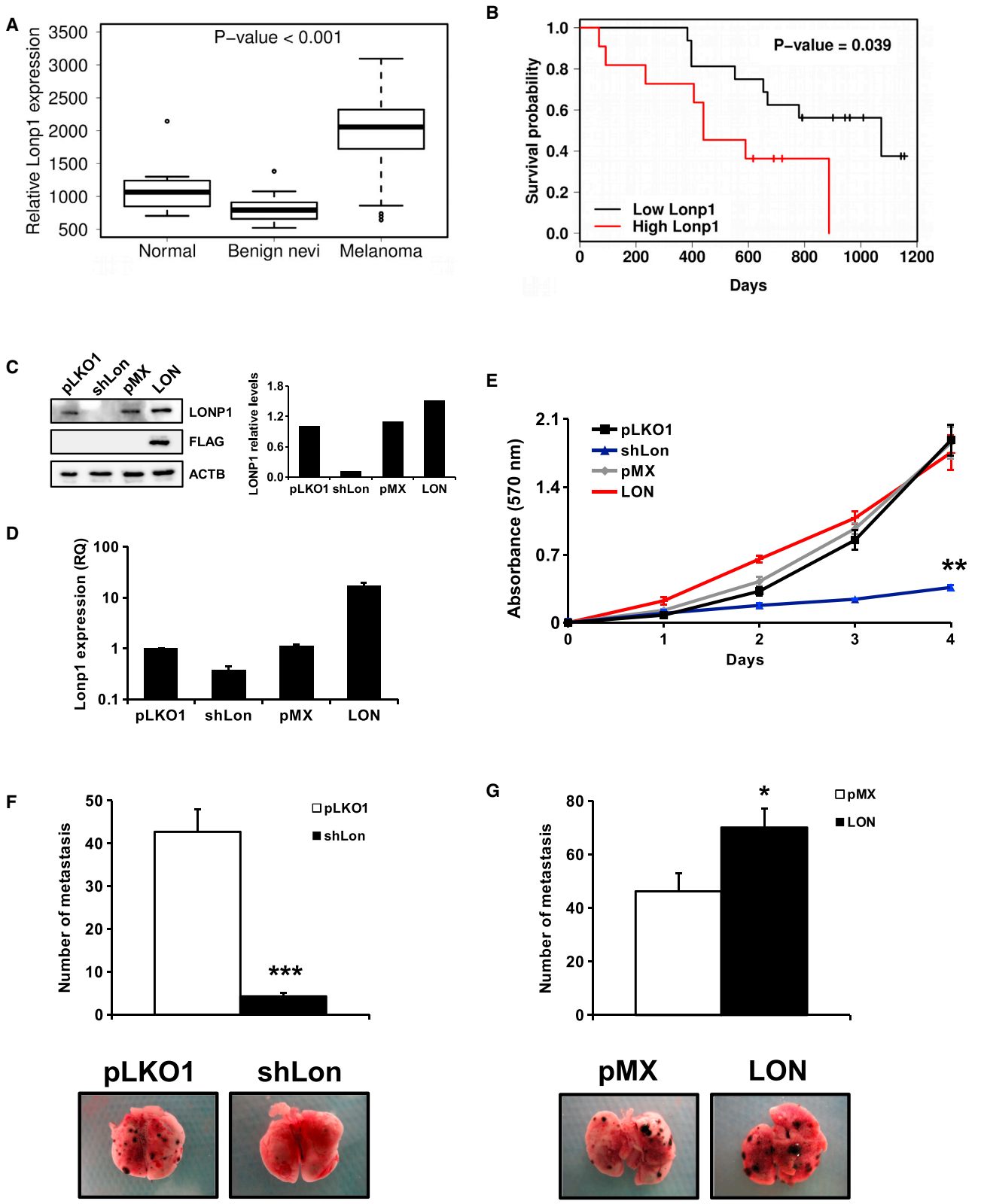

(legend on next page)

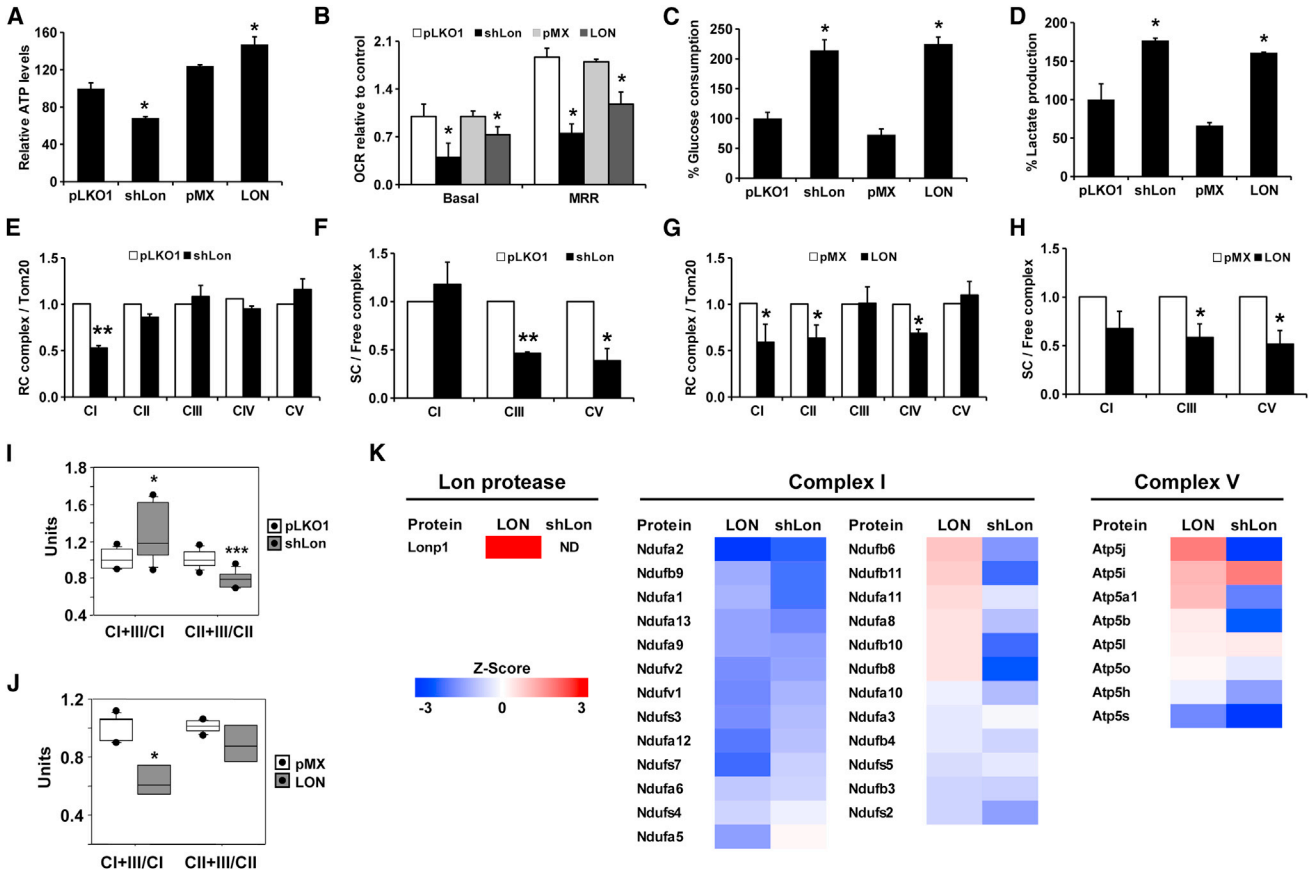

Figure 5. LONP1 Controls Tumor Bioenergetics by Remodeling OXPHOS Subunits

(A–K) B16F10 melanoma cells with knockdown (shLon) and overexpression (LON) of Lon protease and their respective controls pLKO1 and pMX were used to study OXPHOS function. (A) Relative ATP levels of the analyzed cells. (B) Oxygen consumption rate (OCR) in basal conditions and after stimulation with trifluorocarbonylcyanide phenylhydrazone, MRR (maximal respiration rate), represented as OCR per cell relative to each control cell. (C) Percentage of glucose consumption and (D) lactate production during 48 hr, relative to control cells. BNGE quantification of OXPHOS subunits (RC complex) using TOM20 as a loading control of isolated mitochondria from (E) shLon and (G) LON cells, relative to each control. BNGE quantification of complexes contained in SC relative to complex free of isolated mitochondria from (F) shLon and (H) LON cells, relative to each control. Combined mitochondrial complex activities relative to free complexes to assess the use of NADH (CI+III/CI) or FAD electron equivalents (CII+III/CII) in (I) shLon cells and (J) LON cells. All experiments were independently carried out at least three times, using triplicates for each cell line; data are presented as mean ± SEM, *p < 0.05, **p < 0.01, ***p < 0.001. (K) Heatmap showing protein abundance changes in Lon protease and subunits of CI and CV, obtained with high-throughput quantitative proteomics of enriched mitochondrial preparations. The relative abundance changes in LON and shLon cells are expressed using the *Z* score in relation to each control. ND, not determined.

DISCUSSION

We describe herein the generation and phenotypic characterization of mice deficient in the mitochondrial Lon protease, as well as the functional analysis of this ATP-dependent enzyme controlling tumor bioenergetics. We found that mice deficient in LONP1 show a lethal phenotype during gastrulation, a period in which a well-fitted mitochondrial function is required to induce

Figure 4. LONP1 Expression Is Essential for Tumor Development and Metastasis Formation

(A) Relative expression levels of *LONP1* in normal skin, benign nevi, and melanoma from data set GDS1375 (Talantov et al., 2005). Data are presented in box-and-whisker plot format.

(B) Kaplan-Meier survival curves for 27 patients with metastatic melanoma expressing high (top 25% of patients) and low (bottom 25% of patients) *LONP1* levels. GSE19234 (Bogunovic et al., 2009).

(C and D) Analysis of LONP1 levels in B16F10-luc2 cells after lentiviral transduction with a control pLKO1 empty vector and shRNA against Lonp1 (shLon) as wells as after retroviral transduction of LON protease (LON) and empty vector pMX, followed by western blot analysis with densitometry quantification and (D) qPCR represented with a RQ value ± SD. LONP1 levels in the overexpressing cells were the cumulative values of endogenous and flagged construct expression.

(E) MTT analysis showed a decrease in proliferation in shLon B16F10-luc2 cell lines. Data are presented as mean ± SEM, **p < 0.01.

(F and G) Total number of lung metastasis, generated in the left lung, using pLKO1 control and shLon B16F10-luc2 melanoma cells, and (G) pMX control and overexpression of Lon protease (LON). Data are presented as mean ± SEM (n = 10), *p < 0.05, ***p < 0.001. (F and G; bottom) Representative images of lungs at the end of each experiment.

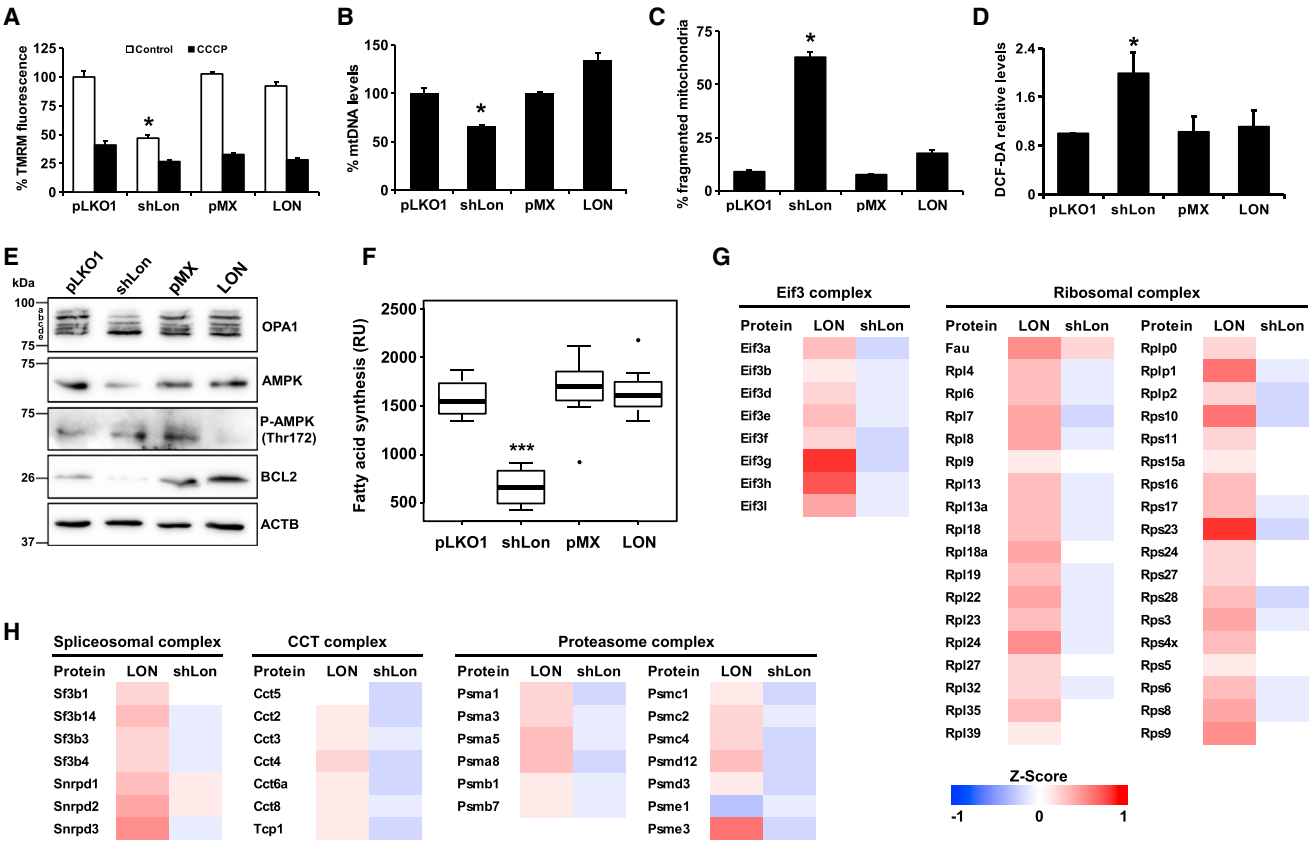

Figure 6. LONP1 Maintains Mitochondrial Function and Promotes a Metabolic Remodeling Process

(A–H) B16F10 melanoma cells with knockdown (shLon) and overexpression of Lon protease (LON) and their respective controls pLKO1 and pMX were used to study mitochondrial function. (A) Mitochondrial membrane potential ($\Delta\Psi m$) represented as a percentage of TMRM fluorescence, in normal cells and after carbonyl cyanide m-chlorophenyl hydrazoneP treatment. (B) mtDNA levels represented as percentage relative to each control. (C) Percentage of fragmented mitochondria quantified after mtDsRed2 transfection. (D) ROS levels represented as relative levels of DCF-DA fluorescence. (E) Western blot analysis showing processing of OPA1 long isoforms (a and b) and increase in the short isoforms (c to e), AMPK activation, and Bcl2 decrease in shLon cells. Overexpression of LON causes reduced AMPK activity and an increase in Bcl2 levels. (F) Fatty acid synthesis rate measured as ^{14}C incorporation into cellular lipids represented as relative units (RU). All experiments were independently carried out at least three times, using triplicates for each condition; data are presented as mean ± SEM, $^{*}p < 0.05$, $^{***}p < 0.001$. Heatmap showing abundance changes of proteins belonging to the eukaryotic translation initiation factor 3 (Eif3) and the ribosomal complexes (G), and to the spliceosome, the proteasome and the chaperone-containing T (CCT) complex (H), obtained with high-throughput quantitative proteomics of whole-cell lysates. The relative abundance changes in LON and shLon cells are expressed using the *Z* score in relation to each control.

profound changes in embryo development (Nagy et al., 2003). At this stage, *Lonp1* null embryos display loss of mtDNA and growth arrest, which are features observed in mice deficient in OXPHOS complex subunits, like GRIM19 and SCO2 (Huang et al., 2004; Yang et al., 2010), or in mtDNA-associated proteins, such as POLG, POLG2, and TFAM (Hance et al., 2005; Humble et al., 2013; Larsson et al., 1998), that also exhibit embryonic lethality. In contrast, *Lonp1*-heterozygous mice develop normally, allowing us to evaluate in vivo the functional and pathological relevance of LONP1 haploinsufficiency. Interestingly, $Lonp1^{+/-}$ mice are protected against chemically induced colorectal and skin tumors, suggesting an oncogenic function for this mitochondrial protease. Consistent with this hypothesis, LONP1 is upregulated in human colorectal and skin carcinomas and their levels are associated with poor clinical outcome of the corresponding patients. Accordingly, *LONP1*-knockdown in colorectal cancer cells reduces in vitro cell proliferation and in vivo growth of tumors derived from these cells, whereas ectopic expression of *LONP1* increases tumor growth. Moreover, overexpression of *LONP1* in melanoma cells increases experimental metastasis formation, whereas knockdown of this protease decreases cell proliferation and lung metastasis. Notably, *LONP1* upregulation does not stimulate cell proliferation, despite the observed increase in tumor growth and metastasis in vivo. The metabolic and stress adaptations undergone by cancer cells during the tumorigenesis process, which are not perfectly replicated in the in vitro experiments, may explain these differences, also observed in similar studies involving other metabolic genes with oncogenic function (Bhalla et al., 2011). Accordingly, we propose that the upregulation of *LONP1* observed in many cancer cell lines and tumor samples (Bernstein et al., 2012; Hu et al., 2005), is probably the consequence of an adaptive metabolic response during malignant transformation.

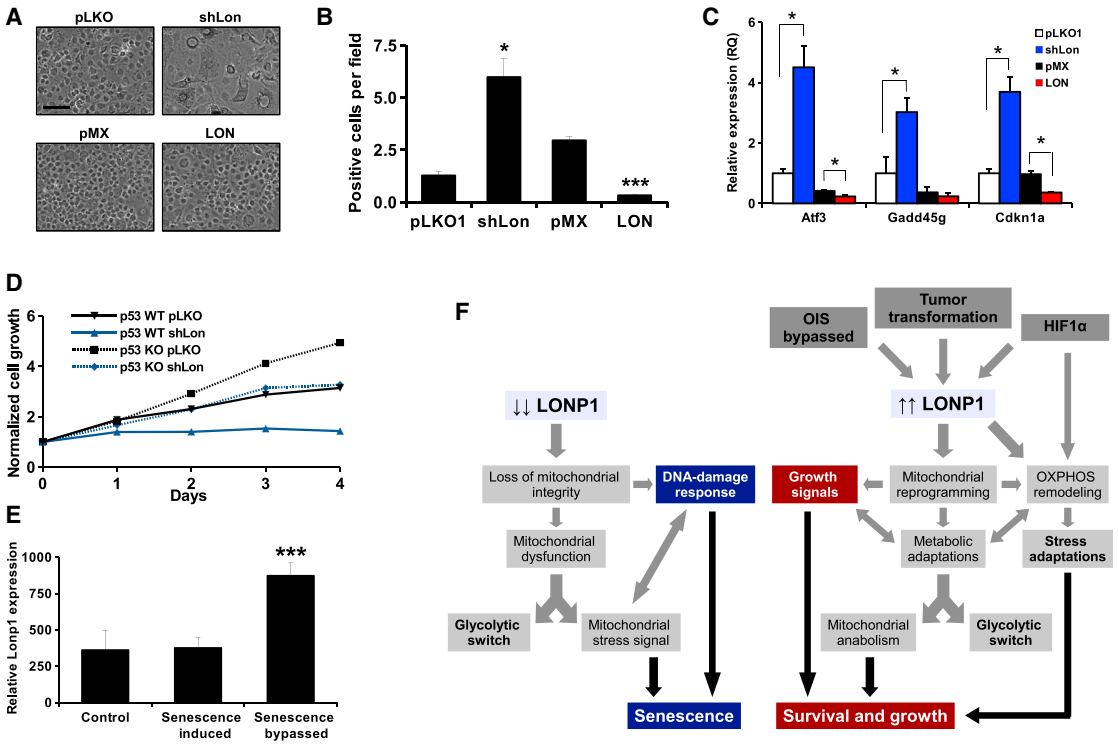

Figure 7. LONP1 Is Necessary to Bypass Oncogene-Induced Senescence

(A) Brightfield images of B16F10 melanoma cells. Scale bar represents 100 μm.

(B) Percentage of cells positive for β-galactosidase activity as a measure of cellular senescence. Data are presented as mean ± SEM, *$p < 0.05$, ***$p < 0.001$.

(C) Transcriptional qPCR analysis of p53-target genes (*Atf3*, *Gadd45 g*, and *Cdkn1a/p21*) in these melanoma cells. Data are shown as RQ value ± SD, *$p < 0.05$.

(D) MTT analysis of *p53*-deficient and wild-type fibroblasts after knockdown of LONP1. The decrease in Lon protease in a background deficient in p53 has less effect than in wild-type background.

(E) *LONP1* relative expression levels in control, senescence-induced, and senescence-bypassed fibroblasts extracted from the data set GSE2484 (Collado et al., 2005). ***$p < 0.001$.

(F) Model summarizing the functional relevance of Lon protease in reprogramming mitochondrial activity in cancer.

Metabolic reprogramming of tumor cells has been recently established as a hallmark of cancer (Hanahan and Weinberg, 2011). Several enzymes have been proposed to act as protumorigenic factors and contribute to this metabolic reprogramming (Chae et al., 2012; Vazquez et al., 2013). Furthermore, mutations in genes encoding mitochondrial and metabolic enzymes have been widely reported in human malignancies (Rodríguez et al., 2013; Yan et al., 2009), indicating that tumor cells harbor genetic alterations that affect metabolic function and facilitate tumor formation. The main feature of this reprogramming process is the switch from oxidative to glycolytic metabolism (Vander Heiden et al., 2009). Curiously, we have found that both upregulation and knockdown of Lon protease in melanoma cells induce the same glycolytic switch, turning cells from oxidative to anaerobic metabolism. In this regard, it is well established that upregulation of the glycolytic pathway during tumor transformation is triggered by oncogenic signals, such as activating mutations in the oncogene *BRAF* in melanoma, as well as by many physiological and pathological conditions which cause metabolic changes (Metallo and Vander Heiden, 2013; Wallace et al., 2010). Additionally, a glycolytic shift is also induced by impairment of the mitochondrial respiratory chain (Hu et al., 2012). This impairment of mitochondrial OXPHOS triggers glycolytic metabolism as a survival mechanism that often ends with cell collapse due to the inability of these damaged cells to reprogram their metabolism (Wallace, 2005). Accordingly, the glycolytic switch observed in cells lacking LONP1 may be an obligate consequence of their mitochondrial dysfunction, not being related to metabolic reprogramming of cancer cells. Conversely, the switch observed in *LONP1*-overexpressing cells is a mitochondria-controlled mechanism, which forms part of a generalized metabolic reprogramming that contributes to the development and progression of cancer.

The metabolic adaptation of shLon cells induces a change in respiration and in the use of electron equivalents, favoring the utilization of NADH electron equivalents feeding CI, which suggests the occurrence of a catabolic phenotype (Lapuente-Brun et al., 2013). However, the decrease in supercomplexes due to loss of specific structural subunits implies that this is not a regulated mechanism, but a consequence of defective assembly or mitochondrial membrane destabilization. In addition, the subsequent loss of membrane potential and the alterations in complex V cause a decrease in ATP generation, whereas the increase in ROS levels exacerbates this mitochondrial dysfunction. These

stress conditions induce the OPA1 processing and mitochondrial fragmentation events that may contribute to the decrease in respiration and functional supercomplexes assembly (Cogliati et al., 2013). Moreover, the loss of mitochondrial membrane potential may inhibit the entry of pyruvate into mitochondria (Herzig et al., 2012), reducing the Krebs cycle function and the generation of essential metabolites for cell viability. Consequently, the decrease in ATP levels and the mitochondrial stress signals induce AMPK activation, which downregulates anabolic pathways, such as lipid synthesis, and upregulates catabolic reactions, such as glycolysis, to try to counteract this stress scenario. However, despite the activation of all these stress-response mechanisms, shLon cells are unable to avoid mitochondrial dysfunction due to the dramatic alterations present in them. Accordingly, the mitochondrial dysfunction in shLon cells activates a genetic damage response, likely mediated by p53, which finally triggers cell cycle arrest and senescence. This response mechanism induced by mitochondrial damage reinforces the role of LONP1 as a guardian against reduced cellular and organismal fitness by contributing to maintain mitochondrial integrity.

Conversely, the glycolytic switch observed in *LONP1*-overexpressing cells is triggered by a regulated metabolic reprogramming, maintaining other mitochondrial functions unaltered. The upregulation of LONP1 induces a remodeling of mitochondrial complexes and supercomplexes, decreasing the mitochondrial respiration and favoring the metabolic switch because, under these conditions, respiratory reactions shift toward the glycolytic pathway (Wallace, 2012). Moreover, Lon protease overexpression reduces the use of NADH equivalents and the respiration through CI, which is frequently mutated and inactivated in tumor cell lines (Santidrian et al., 2013). However, despite the reduction of levels and activity of mitochondrial complexes, LONP1 also increases the stability of the CI basic structure. This conversion indicates that the inactivation is regulated and that remodeling could maintain the ability to activate the respiration to increase metabolic flexibility when it is required, a mechanism that has been proposed in other similar contexts (Dieteren et al., 2012).

Lon protease appears to be a key factor in metabolic reprogramming through remodeling of mitochondrial function, supporting the idea that steady-state alterations of this ATP-dependent protease have a significant impact on respiratory chain activity (Figure 7F). This function is consistent with previous studies showing that LONP1 degrades COX4-1 in response to HIF1a and leads to the exchange of this subunit with COX4-2, which is more effective under hypoxic conditions (Fukuda et al., 2007). Recent studies have also shown that Lon protease overexpression upregulates the CI subunit NDUFS8 and generates a more aggressive phenotype in cancer cells (Cheng et al., 2013). All of these data illustrate the essential roles of LONP1 in the regulation of mitochondrial and OXPHOS function in tumor cells. We have also observed that metabolic reprogramming promoted by LONP1 enhances protein synthesis and metabolism and activates different pathways that may contribute to the observed aggressiveness of cancer cells overexpressing *LONP1*. Nevertheless, because the Lon protease is also increased in response to other stress stimuli (Hori et al., 2002), it is likely that additional proteolytic processing events associated with these stress responses may also contribute to the increased tumorigenesis caused by upregulation of this enzyme. Furthermore, the increase in *LONP1* expression after bypass of OIS highlights the importance of Lon protease in tumor transformation and mitochondrial metabolic reprogramming. Hence, LONP1 emerges as an indispensable protease for cellular life, also being necessary for tumor growth due to its ability to maintain and modulate mitochondrial activity.

In summary, the generation of *Lonp1*-deficient mice has allowed us to identify the essential roles of this mitochondrial protease in cell and organismal viability. Additionally, the identification of LONP1 as a key metabolic factor affecting mitochondrial reprogramming and tumor bioenergetics may open a way to develop cancer therapies. These results confirm the importance of studying genetic and metabolic alterations in tumor cells, in order to rationalize an effective response to anticipate the development of cancer.

EXPERIMENTAL PROCEDURES

Generation of *Lonp1*$^{-/-}$ Mice and Genotyping

The *Lonp1*-heterozygous mice were provided by Texas Institute for Genomic Medicine (Figure S1A). We used genomic DNA from tail samples for PCR genotyping under the following conditions: denaturation at 94°C for 15 s, annealing at 62°C for 15 s, and extension at 72°C for 45 s, 30 cycles. We used the following primers for genotyping: wild-type-specific forward 5′-ccctgactgca gagattgtgaa-3′, mutation-specific forward 5′-caggacatagcgttggctacc-3′, and common reverse 5′-ttcagtgccagtgccttagagt-3′.

Animal Studies and Carcinogenesis Protocols

All animal procedures were approved in accordance with the guidelines of the Committee for Animal Experimentation of the Universidad de Oviedo. Xenograft studies were performed as described (Fraile et al., 2013). Colon and skin carcinogenesis, and lung metastasis were induced as reported (Balbín et al., 2003; Gutiérrez-Fernández et al., 2008; Neufert et al., 2007). Complete methods can be found in the Supplemental Experimental Procedures.

Cell Culture

Cancer cell lines 293T, HCT116, HCT15, HT29, SW480, SW620, DLD-1, RKO, and FHC were purchased from the American Type Culture Collection. The luciferase-expressing cell line B16F10 Luc2 was purchased from Caliper Life Sciences. Cells were routinely maintained in Dulbecco's modified Eagle's medium containing 10% fetal bovine serum, 100 U/ml penicillin, and 100 μg/ml streptomycin (Life Technologies).

DNA Constructs

Mouse cDNA from *LONP1* was cloned tagged with a FLAG epitope in the carboxy terminus and subcloned into the pMX retroviral vector. The construct was verified by capillary sequencing. For RNA interference experiments, five shRNA vectors were purchased for human and mouse *LONP1* (RHS4533-NM_004793 for human and RMM4534-NM_028782 for mouse; Open Biosystems, Thermo Scientific).

Seahorse Analysis of Mitochondrial Function

Oxygen consumption was measured in 2×10^4 intact cells using a Seahorse Bioscience XF96 extracellular flux analyzer, following the manufacturer's instructions. Briefly, after a 12 min equilibration, three measurements of 3 min were performed, separated by 3 min of mixing. Maximal membrane potential was assessed with the addition of 1 μM oligomycin, and uncoupled mitochondrial respiration was induced with injection of 1 μM carbonyl cyanide m-chlorophenyl hydrazone. To stop the mitochondrial-dependent oxygen consumption, both 1 μM rotenone and antimycin were used.

Statistical Analysis

All experimental data are reported as means and the error bars represent SEM. Differences between mean values were analyzed with two-tailed Student's t test, except in the cases that indicate use of another statistical test. A $p < 0.05$ was considered significant and statistically significant differences are shown with asterisks. All statistical analyses were done using LibreOffice or the statistical package R (http://www.r-project.org/) and the application Rstudio (http://www.rstudio.org).

SUPPLEMENTAL INFORMATION

Supplemental Information includes Supplemental Experimental Procedures, five figures, and one table and can be found with this article online at http://dx.doi.org/10.1016/j.celrep.2014.06.018.

ACKNOWLEDGMENTS

We thank J.M. Fraile, J. de la Rosa, A.R. Folgueras, J.M.P. Freije, S. Cal, M. Mittelbrunn, and M.T. Fernández-García for helpful comments and C. Garabaya, A. Moyano, R. Feijoo, I. Martínez, and the Servicio de Histopatología (IUOPA) for excellent technical assistance. This work was supported by grants from the Ministerio de Economía y Competitividad, Instituto de Salud Carlos III (RTICC), and Red Temática de Investigación Cooperativa en Enfermedades Cardiovasculares. The Instituto Universitario de Oncología is supported by Obra Social Cajastur. K.W. is supported by the Strategic Young Researcher Overseas Visits Program for Accelerating Brain Circulation from Japan Society for the Promotion of Science. C.L-O. is an investigator for the Botin Foundation.

Received: August 9, 2013
Revised: March 19, 2014
Accepted: June 12, 2014
Published: July 10, 2014

REFERENCES

Andrews, B., Carroll, J., Ding, S., Fearnley, I.M., and Walker, J.E. (2013). Assembly factors for the membrane arm of human complex I. Proc. Natl. Acad. Sci. USA *110*, 18934–18939.

Balbín, M., Fueyo, A., Tester, A.M., Pendás, A.M., Pitiot, A.S., Astudillo, A., Overall, C.M., Shapiro, S.D., and López-Otín, C. (2003). Loss of collagenase-2 confers increased skin tumor susceptibility to male mice. Nat. Genet. *35*, 252–257.

Bernstein, S.H., Venkatesh, S., Li, M., Lee, J., Lu, B., Hilchey, S.P., Morse, K.M., Metcalfe, H.M., Skalska, J., Andreeff, M., et al. (2012). The mitochondrial ATP-dependent Lon protease: a novel target in lymphoma death mediated by the synthetic triterpenoid CDDO and its derivatives. Blood *119*, 3321–3329.

Bhalla, K., Hwang, B.J., Dewi, R.E., Ou, L., Twaddel, W., Fang, H.-B., Vafai, S.B., Vazquez, F., Puigserver, P., Boros, L., and Girnun, G.D. (2011). PGC1α promotes tumor growth by inducing gene expression programs supporting lipogenesis. Cancer Res. *71*, 6888–6898.

Bogunovic, D., O'Neill, D.W., Belitskaya-Levy, I., Vacic, V., Yu, Y.-L., Adams, S., Darvishian, F., Berman, R., Shapiro, R., Pavlick, A.C., et al. (2009). Immune profile and mitotic index of metastatic melanoma lesions enhance clinical staging in predicting patient survival. Proc. Natl. Acad. Sci. USA *106*, 20429–20434.

Bota, D.A., and Davies, K.J. (2002). Lon protease preferentially degrades oxidized mitochondrial aconitase by an ATP-stimulated mechanism. Nat. Cell Biol. *4*, 674–680.

Bota, D.A., Ngo, J.K., and Davies, K.J. (2005). Downregulation of the human Lon protease impairs mitochondrial structure and function and causes cell death. Free Radic. Biol. Med. *38*, 665–677.

Castle, J.C., Kreiter, S., Diekmann, J., Löwer, M., van de Roemer, N., de Graaf, J., Selmi, A., Diken, M., Boegel, S., Paret, C., et al. (2012). Exploiting the mutanome for tumor vaccination. Cancer Res. *72*, 1081–1091.

Chae, Y.C., Caino, M.C., Lisanti, S., Ghosh, J.C., Dohi, T., Danial, N.N., Villanueva, J., Ferrero, S., Vaira, V., Santambrogio, L., et al. (2012). Control of tumor bioenergetics and survival stress signaling by mitochondrial HSP90s. Cancer Cell *22*, 331–344.

Cheng, C.-W., Kuo, C.-Y., Fan, C.-C., Fang, W.-C., Jiang, S.S., Lo, Y.-K., Wang, T.-Y., Kao, M.-C., and Lee, A.Y.-L. (2013). Overexpression of Lon contributes to survival and aggressive phenotype of cancer cells through mitochondrial complex I-mediated generation of reactive oxygen species. Cell Death Dis. *4*, e681.

Cipolat, S., Rudka, T., Hartmann, D., Costa, V., Serneels, L., Craessaerts, K., Metzger, K., Frezza, C., Annaert, W., D'Adamio, L., et al. (2006). Mitochondrial rhomboid PARL regulates cytochrome c release during apoptosis via OPA1-dependent cristae remodeling. Cell *126*, 163–175.

Cogliati, S., Frezza, C., Soriano, M.E., Varanita, T., Quintana-Cabrera, R., Corrado, M., Cipolat, S., Costa, V., Casarin, A., Gomes, L.C., et al. (2013). Mitochondrial cristae shape determines respiratory chain supercomplexes assembly and respiratory efficiency. Cell *155*, 160–171.

Collado, M., Gil, J., Efeyan, A., Guerra, C., Schuhmacher, A.J., Barradas, M., Benguría, A., Zaballos, A., Flores, J.M., Barbacid, M., et al. (2005). Tumour biology: senescence in premalignant tumours. Nature *436*, 642.

Dieteren, C.E.J., Koopman, W.J.H., Swarts, H.G., Peters, J.G.P., Maczuga, P., van Gemst, J.J., Masereeuw, R., Smeitink, J.A.M., Nijtmans, L.G.J., and Willems, P.H.G.M. (2012). Subunit-specific incorporation efficiency and kinetics in mitochondrial complex I homeostasis. J. Biol. Chem. *287*, 41851–41860.

Fraile, J.M., Quesada, V., Rodríguez, D., Freije, J.M.P., and López-Otín, C. (2012). Deubiquitinases in cancer: new functions and therapeutic options. Oncogene *31*, 2373–2388.

Fraile, J.M., Ordóñez, G.R., Quirós, P.M., Astudillo, A., Galván, J.A., Colomer, D., López-Otín, C., Freije, J.M.P., and Puente, X.S. (2013). Identification of novel tumor suppressor proteases by degradome profiling of colorectal carcinomas. Oncotarget *4*, 1931–1932.

Freije, J.M.P., Fraile, J.M., and López-Otín, C. (2011). Protease addiction and synthetic lethality in cancer. Front Oncol *1*, 25.

Friedman, J.R., and Nunnari, J. (2014). Mitochondrial form and function. Nature *505*, 335–343.

Fukuda, R., Zhang, H., Kim, J.W., Shimoda, L., Dang, C.V., and Semenza, G.L. (2007). HIF-1 regulates cytochrome oxidase subunits to optimize efficiency of respiration in hypoxic cells. Cell *129*, 111–122.

Granot, Z., Kobiler, O., Melamed-Book, N., Eimerl, S., Bahat, A., Lu, B., Braun, S., Maurizi, M.R., Suzuki, C.K., Oppenheim, A.B., and Orly, J. (2007). Turnover of mitochondrial steroidogenic acute regulatory (StAR) protein by Lon protease: the unexpected effect of proteasome inhibitors. Mol. Endocrinol. *21*, 2164–2177.

Gutiérrez-Fernández, A., Fueyo, A., Folgueras, A.R., Garabaya, C., Pennington, C.J., Pilgrim, S., Edwards, D.R., Holliday, D.L., Jones, J.L., Span, P.N., et al. (2008). Matrix metalloproteinase-8 functions as a metastasis suppressor through modulation of tumor cell adhesion and invasion. Cancer Res. *68*, 2755–2763.

Hanahan, D., and Weinberg, R.A. (2011). Hallmarks of cancer: the next generation. Cell *144*, 646–674.

Hance, N., Ekstrand, M.I., and Trifunovic, A. (2005). Mitochondrial DNA polymerase gamma is essential for mammalian embryogenesis. Hum. Mol. Genet. *14*, 1775–1783.

Haq, R., Shoag, J., Andreu-Perez, P., Yokoyama, S., Edelman, H., Rowe, G.C., Frederick, D.T., Hurley, A.D., Nellore, A., Kung, A.L., et al. (2013). Oncogenic BRAF regulates oxidative metabolism via PGC1α and MITF. Cancer Cell *23*, 302–315.

Herzig, S., Raemy, E., Montessuit, S., Veuthey, J.-L., Zamboni, N., Westermann, B., Kunji, E.R.S., and Martinou, J.-C. (2012). Identification and functional expression of the mitochondrial pyruvate carrier. Science *337*, 93–96.

Hori, O., Ichinoda, F., Tamatani, T., Yamaguchi, A., Sato, N., Ozawa, K., Kitao, Y., Miyazaki, M., Harding, H.P., Ron, D., et al. (2002). Transmission of cell

stress from endoplasmic reticulum to mitochondria: enhanced expression of Lon protease. J. Cell Biol. *157*, 1151–1160.

Hu, J., Bianchi, F., Ferguson, M., Cesario, A., Margaritora, S., Granone, P., Goldstraw, P., Tetlow, M., Ratcliffe, C., Nicholson, A.G., et al. (2005). Gene expression signature for angiogenic and nonangiogenic non-small-cell lung cancer. Oncogene *24*, 1212–1219.

Hu, Y., Lu, W., Chen, G., Wang, P., Chen, Z., Zhou, Y., Ogasawara, M., Trachootham, D., Feng, L., Pelicano, H., et al. (2012). K-ras(G12V) transformation leads to mitochondrial dysfunction and a metabolic switch from oxidative phosphorylation to glycolysis. Cell Res. *22*, 399–412.

Huang, G., Lu, H., Hao, A., Ng, D.C.H., Ponniah, S., Guo, K., Lufei, C., Zeng, Q., and Cao, X. (2004). GRIM-19, a cell death regulatory protein, is essential for assembly and function of mitochondrial complex I. Mol. Cell. Biol. *24*, 8447–8456.

Humble, M.M., Young, M.J., Foley, J.F., Pandiri, A.R., Travlos, G.S., and Copeland, W.C. (2013). Polg2 is essential for mammalian embryogenesis and is required for mtDNA maintenance. Hum. Mol. Genet. *22*, 1017–1025.

Jorissen, R.N., Gibbs, P., Christie, M., Prakash, S., Lipton, L., Desai, J., Kerr, D., Aaltonen, L.A., Arango, D., Kruhøffer, M., et al. (2009). Metastasis-associated gene expression changes predict poor outcomes in patients with Dukes stage B and C colorectal cancer. Clin. Cancer Res. *15*, 7642–7651.

Kita, K., Suzuki, T., and Ochi, T. (2012). Diphenylarsinic acid promotes degradation of glutaminase C by mitochondrial Lon protease. J. Biol. Chem. *287*, 18163–18172.

Lapuente-Brun, E., Moreno-Loshuertos, R., Acín-Pérez, R., Latorre-Pellicer, A., Colás, C., Balsa, E., Perales-Clemente, E., Quirós, P.M., Calvo, E., Rodríguez-Hernández, M.A., et al. (2013). Supercomplex assembly determines electron flux in the mitochondrial electron transport chain. Science *340*, 1567–1570.

Larsson, N.G., Wang, J., Wilhelmsson, H., Oldfors, A., Rustin, P., Lewandoski, M., Barsh, G.S., and Clayton, D.A. (1998). Mitochondrial transcription factor A is necessary for mtDNA maintenance and embryogenesis in mice. Nat. Genet. *18*, 231–236.

Lazarou, M., McKenzie, M., Ohtake, A., Thorburn, D.R., and Ryan, M.T. (2007). Analysis of the assembly profiles for mitochondrial- and nuclear-DNA-encoded subunits into complex I. Mol. Cell. Biol. *27*, 4228–4237.

Liu, T., Lu, B., Lee, I., Ondrovicová, G., Kutejová, E., and Suzuki, C.K. (2004). DNA and RNA binding by the mitochondrial lon protease is regulated by nucleotide and protein substrate. J. Biol. Chem. *279*, 13902–13910.

López-Otín, C., Blasco, M.A., Partridge, L., Serrano, M., and Kroemer, G. (2013). The hallmarks of aging. Cell *153*, 1194–1217.

Lu, B., Liu, T., Crosby, J.A., Thomas-Wohlever, J., Lee, I., and Suzuki, C.K. (2003). The ATP-dependent Lon protease of Mus musculus is a DNA-binding protein that is functionally conserved between yeast and mammals. Gene *306*, 45–55.

Lu, B., Lee, J., Nie, X., Li, M., Morozov, Y.I., Venkatesh, S., Bogenhagen, D.F., Temiakov, D., and Suzuki, C.K. (2013). Phosphorylation of human TFAM in mitochondria impairs DNA binding and promotes degradation by the AAA+ Lon protease. Mol. Cell *49*, 121–132.

Matsushima, Y., Goto, Y., and Kaguni, L.S. (2010). Mitochondrial Lon protease regulates mitochondrial DNA copy number and transcription by selective degradation of mitochondrial transcription factor A (TFAM). Proc. Natl. Acad. Sci. USA *107*, 18410–18415.

Metallo, C.M., and Vander Heiden, M.G. (2013). Understanding metabolic regulation and its influence on cell physiology. Mol. Cell *49*, 388–398.

Michaloglou, C., Vredeveld, L.C.W., Soengas, M.S., Denoyelle, C., Kuilman, T., van der Horst, C.M.A.M., Majoor, D.M., Shay, J.W., Mooi, W.J., and Peeper, D.S. (2005). BRAFE600-associated senescence-like cell cycle arrest of human naevi. Nature *436*, 720–724.

Nagy, A., Gertsenstein, M., Vintersten, K., and Behringer, R. (2003). Manipulating the Mouse Embryo: a Laboratory Manual (Woodbury, NY: Cold Spring Harbor Laboratory Press).

Neufert, C., Becker, C., and Neurath, M.F. (2007). An inducible mouse model of colon carcinogenesis for the analysis of sporadic and inflammation-driven tumor progression. Nat. Protoc. *2*, 1998–2004.

Perales-Clemente, E., Fernández-Vizarra, E., Acín-Pérez, R., Movilla, N., Bayona-Bafaluy, M.P., Moreno-Loshuertos, R., Pérez-Martos, A., Fernández-Silva, P., and Enríquez, J.A. (2010). Five entry points of the mitochondrially encoded subunits in mammalian complex I assembly. Mol. Cell. Biol. *30*, 3038–3047.

Quirós, P.M., Ramsay, A.J., Sala, D., Fernández-Vizarra, E., Rodríguez, F., Peinado, J.R., Fernández-García, M.S., Vega, J.A., Enríquez, J.A., Zorzano, A., and López-Otín, C. (2012). Loss of mitochondrial protease OMA1 alters processing of the GTPase OPA1 and causes obesity and defective thermogenesis in mice. EMBO J. *31*, 2117–2133.

Rodríguez, D., Ramsay, A.J., Quesada, V., Garabaya, C., Campo, E., Freije, J.M.P., and López-Otín, C. (2013). Functional analysis of sucrase-isomaltase mutations from chronic lymphocytic leukemia patients. Hum. Mol. Genet. *22*, 2273–2282.

Rugarli, E.I., and Langer, T. (2012). Mitochondrial quality control: a matter of life and death for neurons. EMBO J. *31*, 1336–1349.

Sabates-Bellver, J., Van der Flier, L.G., de Palo, M., Cattaneo, E., Maake, C., Rehrauer, H., Laczko, E., Kurowski, M.A., Bujnicki, J.M., Menigatti, M., et al. (2007). Transcriptome profile of human colorectal adenomas. Mol. Cancer Res. *5*, 1263–1275.

Santidrian, A.F., Matsuno-Yagi, A., Ritland, M., Seo, B.B., LeBoeuf, S.E., Gay, L.J., Yagi, T., and Felding-Habermann, B. (2013). Mitochondrial complex I activity and NAD+/NADH balance regulate breast cancer progression. J. Clin. Invest. *123*, 1068–1081.

Serrano, M., Lin, A.W., McCurrach, M.E., Beach, D., and Lowe, S.W. (1997). Oncogenic ras provokes premature cell senescence associated with accumulation of p53 and p16INK4a. Cell *88*, 593–602.

Talantov, D., Mazumder, A., Yu, J.X., Briggs, T., Jiang, Y., Backus, J., Atkins, D., and Wang, Y. (2005). Novel genes associated with malignant melanoma but not benign melanocytic lesions. Clin. Cancer Res. *11*, 7234–7242.

Tatsuta, T. (2009). Protein quality control in mitochondria. J. Biochem. *146*, 455–461.

Tian, Q., Li, T., Hou, W., Zheng, J., Schrum, L.W., and Bonkovsky, H.L. (2011). Lon peptidase 1 (LONP1)-dependent breakdown of mitochondrial 5-aminolevulinic acid synthase protein by heme in human liver cells. J. Biol. Chem. *286*, 26424–26430.

Vander Heiden, M.G., Cantley, L.C., and Thompson, C.B. (2009). Understanding the Warburg effect: the metabolic requirements of cell proliferation. Science *324*, 1029–1033.

Vazquez, F., Lim, J.-H., Chim, H., Bhalla, K., Girnun, G., Pierce, K., Clish, C.B., Granter, S.R., Widlund, H.R., Spiegelman, B.M., and Puigserver, P. (2013). PGC1α expression defines a subset of human melanoma tumors with increased mitochondrial capacity and resistance to oxidative stress. Cancer Cell *23*, 287–301.

Venkatesh, S., Lee, J., Singh, K., Lee, I., and Suzuki, C.K. (2012). Multitasking in the mitochondrion by the ATP-dependent Lon protease. Biochim. Biophys. Acta *1823*, 56–66.

Wallace, D.C. (2005). A mitochondrial paradigm of metabolic and degenerative diseases, aging, and cancer: a dawn for evolutionary medicine. Annu. Rev. Genet. *39*, 359–407.

Wallace, D.C. (2012). Mitochondria and cancer. Nat. Rev. Cancer *12*, 685–698.

Wallace, D.C., Fan, W., and Procaccio, V. (2010). Mitochondrial energetics and therapeutics. Annu. Rev. Pathol. *5*, 297–348.

Yan, H., Parsons, D.W., Jin, G., McLendon, R., Rasheed, B.A., Yuan, W., Kos, I., Batinic-Haberle, I., Jones, S., Riggins, G.J., et al. (2009). IDH1 and IDH2 mutations in gliomas. N. Engl. J. Med. *360*, 765–773.

Yang, H., Brosel, S., Acin-Perez, R., Slavkovich, V., Nishino, I., Khan, R., Goldberg, I.J., Graziano, J., Manfredi, G., and Schon, E.A. (2010). Analysis of mouse models of cytochrome c oxidase deficiency owing to mutations in Sco2. Hum. Mol. Genet. *19*, 170–180.